



Transport of mercury in the Arctic atmosphere: Evidence for a spring-time net sink and summer-time source

D. Hirdman,¹ K. Aspmo,¹ J. F. Burkhart,¹ S. Eckhardt,¹ H. Sodemann,¹ and A. Stohl¹

Received 25 March 2009; revised 20 May 2009; accepted 27 May 2009; published 26 June 2009.

[1] In the Arctic, atmospheric concentrations of gaseous elemental mercury (GEM) can decrease strongly in spring when mercury is deposited to the snow. Some studies suggest mercury can accumulate in the snow while others suggest rapid reemission after atmospheric mercury depletion events. We have combined measurements of GEM at the Arctic site Zeppelin (Ny Ålesund, Spitsbergen) with the output of the Lagrangian particle dispersion model FLEXPART, for a statistical analysis of GEM source and sink regions. We find that the Arctic is a strong net sink region for GEM in April and May, suggesting that mercury accumulates in the Arctic snow pack. For summer, we find the Arctic to be a GEM source, indicating reemission of previously deposited mercury when the snow and/or ice melts, or evasion from the ocean through sea ice leads and polynyas. Our results are corroborated by a related analysis of ozone source and sink regions. **Citation:** Hirdman, D., K. Aspmo, J. F. Burkhart, S. Eckhardt, H. Sodemann, and A. Stohl (2009), Transport of mercury in the Arctic atmosphere: Evidence for a spring-time net sink and summer-time source, *Geophys. Res. Lett.*, 36, L12814, doi:10.1029/2009GL038345.

1. Introduction

[2] Mercury (Hg) is emitted to the atmosphere by a variety of natural (volcanoes, wildfires, etc.) and anthropogenic (e.g., combustion of coal) sources. While anthropogenic Hg emissions have decreased over North America and Europe during the 1990s, emissions in Asia have increased strongly and China is now the country with the by far largest Hg emissions worldwide [Pacyna *et al.*, 2006]. In the atmosphere, Hg exists predominantly as gaseous elemental mercury (GEM) which under normal conditions has an atmospheric lifetime of 6–24 months [Schroeder and Munthe, 1998]. Consequently, GEM can be transported over long distances and is quite uniformly distributed in a hemisphere but has substantial interhemispheric concentration differences. GEM can be converted to various oxidized compounds in the gas or particulate phase, which have a much shorter atmospheric lifetime than GEM. These compounds can be deposited rapidly to the Earth's surface but previously deposited Hg can also be remitted by evasion of GEM.

[3] During so-called atmospheric mercury depletion events (AMDEs), which occur in the Arctic during the spring, GEM concentrations can decrease substantially, despite the otherwise long lifetime of GEM [Schroeder *et al.*, 1998]. AMDEs are accompanied by ozone (O_3) deple-

tion events (ODEs), which are caused by strong emissions of halogen compounds and a catalytic cycling of ozone-destroying halogen atoms and radicals [McConnell *et al.*, 1992], now often termed bromine explosions. Reactions with Br atoms or BrO radicals also oxidize GEM to reactive gaseous mercury, which is then deposited to snow or ice in the Arctic [Lindberg *et al.*, 2002]. The fate of Hg in the snow pack, however, is still heavily discussed. Some studies suggest that Hg deposited during AMDEs in spring accumulates in the snow and is later released with melt water in a form that is available to biota [e.g., Lindberg *et al.*, 2002]. Other studies suggest that in the snow Hg is reduced and remitted to the atmosphere as GEM within a few days after deposition, without any sign of accumulation in the snow pack [e.g., Lalonde *et al.*, 2002; Steffen *et al.*, 2002]. GEM concentrations in the Arctic are highest in summer, which has been attributed to release of Hg previously deposited in spring [Steffen *et al.*, 2005] and/or evasion of GEM from the ocean through open leads [Aspmo *et al.*, 2006].

[4] In this study, we present a statistical analysis of the source regions of GEM observed at an Arctic observatory. We demonstrate strong overall influence of AMDEs on spring-time GEM levels, indicating that a substantial amount of GEM must be removed from the atmosphere at least for some months. In addition, we show that measured GEM concentrations in summer are systematically enhanced by GEM emissions in the Arctic, either by reemission of previously deposited Hg during melting, or from the ocean.

2. Methods

[5] For our analysis, we use measurement data from the research station Zeppelin (11.9°E, 78.9°N, 478 m asl). The station is situated in an unperturbed Arctic environment on a ridge of Zeppelin mountain on the western coast of Spitsbergen. The station is accessible via cable car from the nearby small settlement of Ny Alesund located near sea level. Contamination of the measurements by emissions from the settlement is minimal because of the altitude difference and the generally stable atmospheric stratification. The station is ideally located for our purpose because air masses arriving with a southwesterly flow from the ice-free North Atlantic Ocean provide a strong contrast to the air masses arriving from the ice-covered Arctic Ocean. Hourly O_3 concentrations were recorded by UV absorption spectrometry (API 400A). GEM measurements with 5 min time resolution were started in February 2000 using a Tekran gas phase mercury analyzer (Model 2537A; Tekran Inc., Toronto, Canada). For more details on GEM measurements at Zeppelin, see Berg *et al.* [2003]. All GEM (and O_3) data obtained during the years 2000–2008 (2000–2007, for

¹Norwegian Institute for Air Research, Kjeller, Norway.

O_3) were averaged to 3 hours, to fit with the time resolution of our model results.

[6] To identify the sources of the measured GEM, we use 3-hourly backward simulations with the Lagrangian particle dispersion model FLEXPART [Stohl *et al.*, 1998, 2005]. FLEXPART was driven with 3-hourly operational meteorological data from the European Centre for Medium-Range Weather Forecasts with $1^\circ \times 1^\circ$ resolution. The model calculates the trajectories of tracer particles using the mean winds from the analysis fields with additional random motions representing turbulence [Stohl and Thomson, 1999] and convection [Forster *et al.*, 2007]. During every 3-hour interval, 40000 particles were released at the measurement point and followed backward for 20 days to calculate an emission sensitivity S on a $1^\circ \times 1^\circ$ grid, under the assumption that removal processes can be neglected. S (in units of s m^{-3}) in a particular grid cell is proportional to the particle residence time in that cell and measures the simulated concentration at the receptor that a source of unit strength (1 kg s^{-1}) in the cell would produce. We use the S distribution in a 100 m layer adjacent to the surface (so-called footprint layer) as input to our statistical analyses of surface sources and sinks.

[7] We use a statistical method to identify possible source and sink regions of GEM based on the measurement data and the model output. The method is similar to older methods based on trajectory calculations [Ashbaugh, 1983; Ashbaugh *et al.*, 1985] but takes advantage of the superior quality of FLEXPART emission sensitivity fields compared to simple trajectories, which ignore turbulence and convection. We relate every one of M measurements to a corresponding modeled footprint emission sensitivity field S and calculate the average

$$S_T(i,j) = \frac{1}{M} \sum_{m=1}^M S(i,j,m), \quad (1)$$

where i, j are grid indices of S . Then we select the subset of the data with the $L = \frac{M}{10}$ highest 10% (or, respectively, lowest 10%) of measured GEM concentrations and calculate

$$S_P(i,j) = \frac{1}{L} \sum_{l=1}^L S(i,j,l), \quad (2)$$

where the suffix P can be either 10 or 90 and indicates the percentile. The ratio

$$R_P(i,j) = \frac{L}{M} \frac{S_P(i,j)}{S_T(i,j)}, \quad (3)$$

with P being again either 10 or 90, can then be used for identifying grid cells that are likely sources (or sinks) of GEM. If air mass transport patterns were the same for the data subset and for the full data set, we would expect $R_P(i,j) = 0.1$ for all i, j . Information on sources and sinks of GEM are contained in the deviations from this expected value. When using the top decile of the data, for instance, $R_{90}(i,j) > 0.1$ means that high measured GEM concentrations are associated preferentially with high S values in grid cell (i,j) , indicating a likely source, whereas $R_{90}(i,j) < 0.1$ indicates a possible sink or at least the absence of a source. Conversely,

when using the lowest decile of the data, $R_{10}(i,j) > 0.1$ indicates a likely sink in grid cell (i,j) , and $R_{10}(i,j) < 0.1$ a source.

[8] Not all features of R_P are statistically significant. Particularly where S_T values are low, spurious R_P values can occur. Therefore, we limit the calculation of R_P to grid cells where $S_T > 5 \cdot 10^{-9} \text{ s m}^{-3}$. We furthermore employ a bootstrap resampling analysis [Devore and Farnum, 1999] to identify non-significant values at the 90% level, which are then iteratively removed by smoothing the R_P field until all values are statistically significant. Bootstrapping was also used by Vasconcelos *et al.* [1996] to determine statistical significance of trajectory statistics.

3. Results

[9] In Figure 1 we show R_P fields for both the highest and the lowest 10% of all GEM data, for three different seasons. In winter, high GEM concentrations (Figure 1a) are associated with transport especially from Europe where R_{90} values exceed 0.25, indicating direct transport of anthropogenic GEM emissions. The R_{10} values in winter (Figure 1d) are below 0.1 almost everywhere. This indicates that air masses associated with low GEM concentrations avoid surface contact and, therefore, must descend from above the boundary layer. The highest R_{10} values (still mostly not exceeding 0.1) are found over the Arctic where there are no emission sources. Given that China has the largest anthropogenic GEM emissions, one would expect China to appear as a source region. However, transport from China is too infrequent on the 20-day time scale of the FLEXPART calculations to be represented in our statistics.

[10] In spring, the picture changes dramatically, especially for the low GEM concentrations. While the R_{90} values are again highest over the middle latitudes (Figure 1b), the lowest 10% of the GEM data are strongly associated with transport across the sea-ice-covered Arctic Ocean at low altitudes (Figure 1e). This is also exactly the area where elevated BrO concentrations are seen in satellite observations during bromine explosions in spring [see, e.g., Lindberg *et al.*, 2002]. Values of $R_{10} > 0.5$ over the Arctic mean that, during spring, low-level transport across the sea ice almost always leads to AMDEs that can be observed at Zeppelin.

[11] In summer, the situation reverses compared to spring. Now high R_{90} values can be found over the Arctic Ocean (Figure 1c), indicating that air masses receive GEM emissions during low-level transport across the Arctic Ocean. On the other hand, no clear GEM sink regions can be found in the $R_{10} < 0.1$ patterns and surface contact in the Arctic is rather avoided (Figure 1f).

[12] For our statistical analyses, we have selected the months of the year for which the seasonal patterns are most pronounced. March is somewhat similar to April and May but the spring-time pattern is not yet fully established. June is a month where both the top and the bottom percentile of GEM concentrations are associated with frequent low-level transport across the Arctic, indicating a switch from the Arctic being a GEM sink to the Arctic being a GEM source. September–November are transition months where no clear R_P patterns can be found.

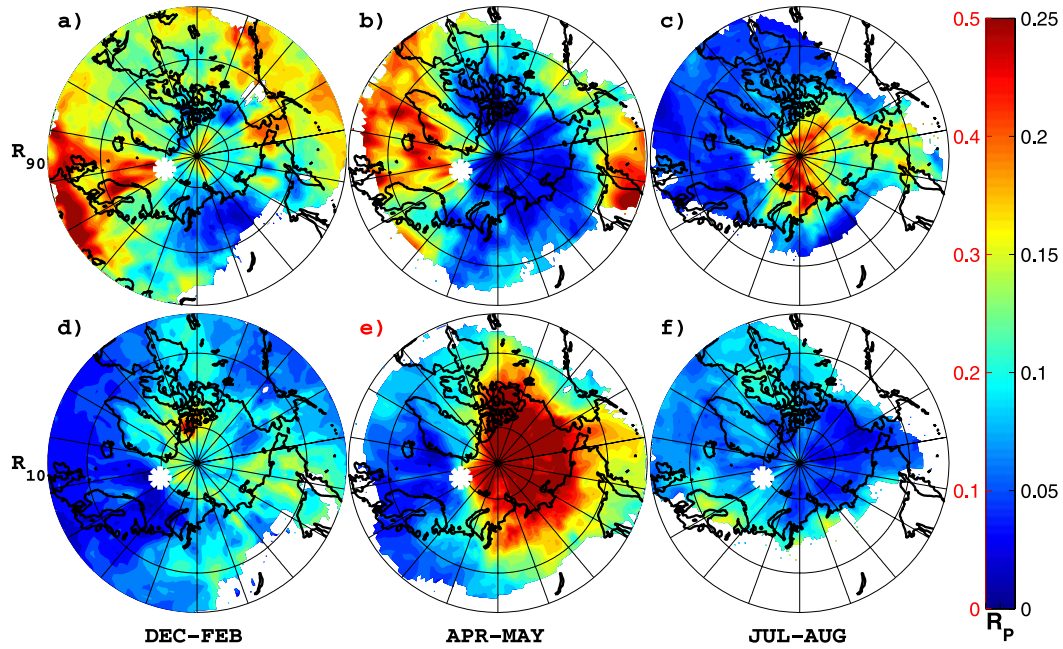


Figure 1. Fields of (a–c) R_{90} and (d–f) R_{10} for GEM measurements at the Zeppelin station during the years 2000–2008, for December–February (Figures 1a and 1d), April–May (Figures 1b and 1e) and July–August (Figures 1c and 1f). Right scale of color bar applies to Figures 1a–1d and 1f, left scale applies to Figure 1e. The white asterisk marks the location of the Zeppelin station. Areas where S_T is below the threshold are plotted white.

[13] Note that our results are insensitive to changes in the data thresholds. Using the top and bottom 20% of the data, for instance, yields almost identical patterns. We have also employed a different statistical analysis that is not based on percentiles but uses the entire dataset and weighs the individual S fields with the corresponding measured GEM concentrations. Again, the Arctic appeared as a sink of GEM in spring and a source in summer. Finally, we have determined the 10% cases with the highest (intense Arctic surface contact) and 10% cases with the lowest (little or no Arctic surface contact) footprint S values aggregated over the entire Arctic Ocean and calculated their respective mean GEM concentrations. This reveals that in April and May air masses having intense surface contact in the Arctic are associated with 33% lower average GEM concentrations ($1.21 \pm 0.19 \text{ ng m}^{-3}$) than air masses having little or no surface contact in the Arctic ($1.83 \pm 0.32 \text{ ng m}^{-3}$). In contrast, in July and August, the average GEM concentrations are higher for air masses having intense surface contact in the Arctic ($1.81 \pm 0.17 \text{ ng m}^{-3}$) than for air masses having little or no contact with the Arctic surface ($1.60 \pm 0.17 \text{ ng m}^{-3}$). In all other months, differences between these two types of air masses are less than 0.07 ng m^{-3} , except for November (0.13 ng m^{-3}).

[14] Our results for spring indicate a net removal of GEM by AMDEs on the seasonal timescale. While past studies have shown that reemission of GEM from the snow pack or sea ice can occur [e.g., Lalonde *et al.*, 2002; Steffen *et al.*, 2002], according to our results not all Hg deposited can be remitted in spring. If all deposited Hg were remitted in the same season, the Arctic would also be associated with high R_{90} values. Furthermore, no net effect on average GEM concentrations would be seen for air masses with intense surface contact in the Arctic. Since we see a 33% reduction

of average GEM concentrations and no GEM concentrations in the top decile for these air masses, our results suggest a net removal of GEM from the atmosphere in the Arctic during spring. This strongly supports the idea that a substantial fraction of Hg removed during AMDEs indeed accumulates in the snow [e.g., Lindberg *et al.*, 2002] and is in agreement with a study conducted at Barrow [Brooks *et al.*, 2006] that showed that during a two-week spring period 60% of the deposited Hg was re-emitted as GEM while 40% remained in the snow.

[15] It is tempting to interpret the GEM source in the Arctic in summer as reemission of Hg deposited during spring. The Arctic GEM source maximizes in July and August and is not evident anymore in September when the ice-free ocean area is larger, possibly indicating that the GEM source is associated with a high rate of melting of snow and sea ice in the Arctic in summer. It has also been shown that underneath the sea ice the surface waters of the Arctic Ocean are supersaturated with dissolved gaseous mercury [Andersson *et al.*, 2008]. The sea ice normally prevents evasion of Hg into the atmosphere, but Aspmo *et al.* [2006] have shown that large Hg fluxes can occur through open leads and polynyas when the sea ice breaks in summer. Thus, the probably more likely explanation for the large GEM source in the Arctic in summer is evasion from the ocean.

[16] To further support the validity of our results, we repeated our statistical analysis for O_3 . Ozone depletion events in spring are highly correlated to those of GEM, but O_3 as no important Arctic sources in summer. Figure 2d shows that in winter low O_3 concentrations are associated with transport from Europe, a result of O_3 titration by anthropogenic nitric oxide emissions. High O_3 concentrations in winter (Figure 2a) and spring (Figure 2b) are

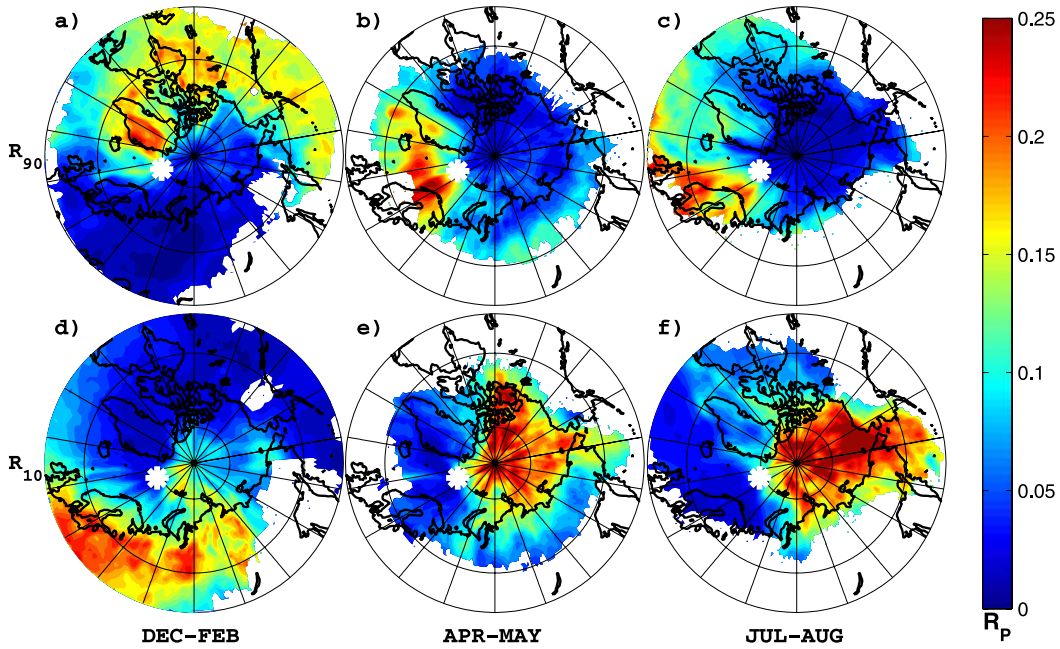


Figure 2. Same as Figure 1 but for ozone for the years 2000–2007.

associated primarily with downward transport from the free troposphere. In winter, this can be seen most clearly by values $R_{90} > 0.2$ over the high topography of Greenland and values $R_{90} < 0.05$ over most low-lying regions (especially those with frequent transport to Zeppelin, not shown). Thus, air masses rich in O_3 tend to have little surface contact.

[17] In spring, low O_3 concentrations are associated with low-level transport across the Arctic Ocean (Figure 2e), indicating the common occurrence of ODEs and AMDEs. In contrast to GEM, however, low O_3 concentrations in summer are associated even more strongly with transport across the Arctic (Figure 2f). In the absence of nitrogen oxide sources, O_3 is quickly destroyed in the relatively moist Arctic boundary layer even without involving halogen chemistry. Furthermore, O_3 formation over the continents in spring and summer (as seen by high R_{90} values over Europe in Figures 2b and 2c) creates a marked contrast to the largely emission-free Arctic. In summary, our results for O_3 show the expected seasonally varying source and sink regions: Europe turning from a sink in winter to a source in summer, the Arctic being a sink during spring and summer, and downward transport from the free troposphere being a source throughout the year, and particularly during winter and spring. This lends confidence also to the source and sink areas we have identified in our analysis of the GEM data.

4. Conclusions

[18] We have used measurements of gaseous elemental mercury (GEM) and ozone at the Arctic measurement site Zeppelin, Ny Ålesund, on Spitsbergen in combination with a Lagrangian particle dispersion model to perform a statistical analysis of the source and sink regions of GEM and ozone. Our conclusions from this study are as follows:

[19] 1. In winter, transport of anthropogenic GEM emissions from mid-latitude source regions (especially Europe)

leads to the highest observed GEM concentrations at Zeppelin. Low GEM concentrations are associated with downward transport of air masses from the free troposphere.

[20] 2. In April and May, high measured GEM concentrations are associated with transport from mid-latitude source regions. Low GEM concentrations are strongly associated with low-level transport across the Arctic Ocean, providing evidence for the influence of atmospheric mercury depletion events (AMDEs) at Zeppelin as reported previously [Berg *et al.*, 2003]. Average GEM concentrations in air masses with strong Arctic Ocean surface contact are 33% lower than in air masses having little or no such contact, showing a net removal of GEM from the air during April and May. Apparently, not all mercury deposited during AMDEs can be reemitted as GEM during the same season. This supports the view that mercury accumulates in the snow pack during spring [Lindberg *et al.*, 2002; Brooks *et al.*, 2006]. Only a fraction of the mercury deposited during AMDEs can be immediately reemitted as suggested by Lalonde *et al.* [2002].

[21] 3. In July and August, the highest measured GEM concentrations are associated with strong surface contact over the Arctic Ocean. This can be explained by reemission of previously deposited mercury when snow melts in summer, and/or by the evasion of GEM from the ocean (which is supersaturated with dissolved gaseous mercury) when the sea ice breaks and direct contact between ocean and atmosphere is facilitated.

[22] 4. A statistical analysis for ozone revealed that in spring low ozone concentrations are found in air masses having ice contact, indicating a common occurrence of ODEs and AMDEs. However, in summer ozone continues to be low in air masses with surface contact in the Arctic Ocean, as expected. For ozone, it is also seen that Europe acts as a sink region in winter (explained by ozone titration) and as a source region in summer (explained by photochemical ozone formation). These easily interpretable

results for ozone support the validity of our statistical transport analyses.

[23] **Acknowledgments.** Two anonymous reviewers provided thoughtful comments on the paper. We thank ECMWF and met.no for access to the ECMWF archives. Funding for this study was provided by the Norwegian Research Council through the POLARCAT project.

References

Andersson, M. E., J. Sommar, K. Gardfeldt, and O. Lindqvist (2008), Enhanced concentrations of dissolved gaseous mercury in the surface waters of the Arctic Ocean, *Mar. Chem.*, **110**, 190–194.

Ashbaugh, L. L. (1983), A statistical trajectory technique for determining air pollution source regions, *J. Air Pollut. Control Assoc.*, **33**, 1096–1098.

Ashbaugh, L. L., W. C. Malm, and W. Z. Sadeh (1985), A residence time probability analysis of sulfur concentrations at Grand Canyon National Park, *Atmos. Environ.*, **19**, 1263–1270.

Aspmo, K., C. Temme, T. Berg, C. Ferrari, P.-A. Gauchard, X. Fain, and G. Wibetoe (2006), Mercury in the atmosphere, snow and melt water ponds in the North Atlantic Ocean during Arctic summer, *Environ. Sci. Technol.*, **40**, 4083–4089.

Berg, T., S. Sekkester, E. Steinnes, A.-K. Valdal, and G. Wibetoe (2003), Springtime depletion of mercury in the European Arctic as observed at Svalbard, *Sci. Total Environ.*, **304**, 43–51.

Brooks, S. B., A. Saiz-Lopez, H. Skov, S. E. Lindberg, J. M. C. Plane, and M. E. Goodsite (2006), The mass balance of mercury in the springtime arctic environment, *Geophys. Res. Lett.*, **33**, L13812, doi:10.1029/2005GL025525.

Devore, J., and N. Farnum (1999), *Applied Statistics for Engineers and Scientists*, pp. 315–318, Duxbury, Pacific Grove, Calif.

Forster, C., A. Stohl, and P. Seibert (2007), Parameterization of convective transport in a Lagrangian particle dispersion model and its evaluation, *J. Appl. Meteorol. Climatol.*, **46**, 403–422.

Lalonde, J. D., A. J. Poulain, and M. Amyot (2002), The role of mercury redox reactions in snow on snow-to-air mercury transfer, *Environ. Sci. Technol.*, **36**, 174–178.

Lindberg, S. E., S. Brooks, C.-J. Lin, K. J. Scott, M. S. Landis, R. K. Stevens, M. Goodsite, and A. Richter (2002), Dynamic oxidation of gaseous mercury in the Arctic troposphere at polar sunrise, *Environ. Sci. Technol.*, **36**, 1245–1256.

McConnell, J. C., G. S. Henderson, L. Barrie, J. Bottenheim, H. Niki, C. H. Langford, and E. M. J. Templeton (1992), Photochemical bromine production implicated in Arctic boundary-layer ozone depletion, *Nature*, **355**, 150–152.

Pacyna, E. G., J. M. Pacyna, F. Steenhuizen, and S. Wilson (2006), Global anthropogenic mercury emission inventory for 2000, *Atmos. Environ.*, **40**, 4048–4063.

Schroeder, W. H., and J. Munthe (1998), Atmospheric mercury—An overview, *Atmos. Environ.*, **32**, 809–822.

Schroeder, W. H., K. G. Anlauf, L. A. Barrie, J. Y. Lu, A. Steffen, D. R. Schneeberger, and T. Berg (1998), Arctic springtime depletion of mercury, *Nature*, **394**, 331–332.

Steffen, A., W. Schroeder, J. Bottenheim, J. Narayan, and J. D. Fuentes (2002), Atmospheric mercury concentrations: Measurements and profiles near snow and ice surfaces in the Canadian Arctic during Alert 2000, *Atmos. Environ.*, **36**, 2653–2661.

Steffen, A., W. Schroeder, R. Macdonald, L. Poissant, and A. Konoplev (2005), Mercury in the Arctic atmosphere: An analysis of eight years of measurements of GEM at Alert (Canada) and a comparison with observations at Amderma (Russia) and Kuujjuaqapik (Canada), *Sci. Total Environ.*, **342**, 185–198.

Stohl, A., and D. J. Thomson (1999), A density correction for Lagrangian particle dispersion models, *Boundary Layer Meteorol.*, **90**, 155–167.

Stohl, A., M. Hittenberger, and G. Wotawa (1998), Validation of the Lagrangian particle dispersion model FLEXPART against large scale tracer experiment data, *Atmos. Environ.*, **32**, 4245–4264.

Stohl, A., C. Forster, A. Frank, P. Seibert, and G. Wotawa (2005), Technical note: The Lagrangian particle dispersion model FLEXPART version 6.2., *Atmos. Chem. Phys.*, **5**, 2461–2474.

Vasconcelos, L. A.d.P., J. D. W. Kahl, D. Liu, E. S. Macias, and W. H. White (1996), A tracer calibration of back trajectory analysis at the Grand Canyon, *J. Geophys. Res.*, **101**, 19,329–19,335.

K. Aspmo, J. F. Burkhart, S. Eckhardt, D. Hirdman, H. Sodemann, and A. Stohl, Norwegian Institute for Air Research, Instituttveien 18, N-2027 Kjeller, Norway. (dhi@nilu.no)